Pharmacy Faculty Articles and Research   School of Pharmacy

9-2005

A Mechanism for the Formation of Nanostructured NiZn Ferrites via a Microemulsion-Assisted Precipitation Method

Vuk Uskoković
Chapman University, uskokovi@chapman.edu

Miha Drofenik
Jožef Štefan Institute

A Mechanism for the Formation of Nanostructured NiZn Ferrites via a Microemulsion-Assisted Precipitation Method

Comments

Creative Commons License

Copyright

A Mechanism for the Formation of Nanostructured NiZn Ferrites via a Microemulsion-Assisted Precipitation Method

Vuk Uskoković[*], **Miha Drofenik**[*, **]

[*] Jožef Stefan Institute, Jamova 39, 1000 Ljubljana, Slovenia
[**] Faculty of Chemistry and Chemical Engineering, Smetanova 17, 2000 Maribor, Slovenia

Corresponding author: Vuk Uskoković, vuk.uskokovic@ijs.si

Abstract

Nanostructured NiZn ferrites were synthesized using two different techniques: first, a precipitation procedure in the reverse micelles of a CTAB/1-hexanol/H_2O microemulsion, and second, precipitation in a bulk aqueous solution. XRD measurements, magnetic measurements, TEM imaging, analytical measurements and thermal analyses were used in an attempt to reveal the chemical pathway that leads to the formation of NiZn ferrite in the microemulsion and in the bulk aqueous solution. It was found that reverse micelles do not act as inert nano-sized reactors that influence only morphological properties of the synthesized powders, but have a decisive influence on the identity of the final product when compared to the non-microemulsion procedure, and therefore present the molecular structures which are actively engaged in the chemical pathway according to which the herein presented room-temperature synthesis of NiZn-ferrite nanoparticles takes place. The influence of the initial pH on the chemical pathway of reverse-micellar synthesis and the morphology of the synthesized particles was discussed after initially it was found that the pH of the precipitation ought to be higher than 8 in order to obtain the desired ferrite as a final product.

Introduction

The reverse-micelles synthesis of materials has recently been attracting much attention, mostly because nanostructured materials with designable particle sizes and uniformly de-agglomerated particle morphologies can be relatively easily prepared using such a technique [1]. In addition to research focused on the synthesis of various nanomaterials within reverse-micellar microemulsions, many studies have looked at modeling and/or theoretically predicting the kinetics of the chemical reactions that occur in reverse-micellar domains [2].

In this study we have compared the synthesis of nanostructured NiZn ferrites produced in reverse-micellar microemulsions with a similar chemical procedure performed in bulk conditions. The crystallization pathways from the supersaturated solutions are generally influenced by a number of factors [3], including foreign surfaces, surface-active agents, the pH, and the level of supersaturation. Also, when synthesizing iron compounds using a wet low-temperature method, the identities of the end products are largely affected by the oxidation rate, the pH and the structure and composition of the initial and intermediate iron species. Considering these effects, it is quite natural to expect that the pathway that leads to the formation of spinel ferrites as part of the

precipitation procedure would normally be different when performed in a reverse-micellar microemulsion than in ordinary bulk solutions.

Experimental

The following chemicals were used in the procedure: $FeSO_4 \cdot 7H_2O$ (>99%, Alfa Aesar), $NiSO_4 \cdot 7H_2O$ (99.7%, Podnart), $ZnSO_4 \cdot 7H_2O$ (>99%, Alfa Aesar) as precursor salts; CTAB (>99%, Alfa Aesar) as the surfactant; 1-hexanol (>98%, Merck-Schuchardt) as the oil phase; de-ionized water as the aqueous phase; $(CH_3)_4NOH$ (25 wt %, 99.5% purity, Alfa Aesar) as the precipitating agent; H_2O_2 (30 wt %, Carlo Erba) as the oxidizing agent; H_2SO_4 (99.8 %, Carlo Erba) as the acidifying agent; and ethanol (99.8 %, Carlo Erba) and de-ionized water as the washing substances. A multi-microemulsion approach was followed. The first reverse-micellar microemulsion in every synthesizing procedure comprised an acidified (to pH = 1.6–1.8 by 1-M H_2SO_4 in order to prevent oxidation of the Fe^{2+} species and subsequent precipitation of the yellow-gray $FeOHSO_4$, which at room temperature and at the concentration used in these experiments occurs at pH ≥ 1.8) 0.237-M aqueous solution of precursor cations (Fe^{2+}, Ni^+, Zn^{2+}), whereas the second microemulsion, which had the same composition as the first, used a 0.5-M aqueous solution of $(CH_3)_4NOH$ as the alkali precipitating agent. The two microemulsions with the same weight composition of CTAB : 1-hexanol : H_2O = 30 : 55 : 15 were mixed and aged for 1 hour (if not denoted for longer times later in the paper) at room temperature. The segregation of phases was not observed, so the agglomeration of the particles occurred during their removal from the parent microemulsion. The colloidal precipitate was sedimented by centrifuging (3 min, 3500 rpm) and repeated washing with ethanol and de-ionized water. The powder was then dried in air at 60^oC, and subsequently characterized. Measurements of pH values during the aging times of the mixed precursor and precipitating microemulsions were performed by using a *Metrohm 691* pH-meter, with the apparatus-indicated values referring not to pH of the aqueous phase (the close medium of the induced chemical recombinations), but to resulting pH of an overall microemulsion system. The produced nanoparticles were investigated using transmission electron microscopy (*JEOL JEM-2000FX*), X-ray diffraction analyses (*D4 Endeavour*), specific magnetization measurements (*MANICS DSM10*). The stoichiometry of the synthesized powders was determined using atomic spectroscopy measurements. The Debye-Scherrer equation was used to evaluate the average particle sizes of the synthesized particles.

Results and discussion

The influence of the reverse micelles on the identity of the final product

The XRD patterns of two different powders synthesized at the same precipitating pH = 12, one in bulk conditions, and the other within the reverse-micellar composition range of the CTAB/1-hexanol/H_2O microemulsion, are shown in Fig. 1. In the latter case, a spinel phase that corresponds to the NiZn-ferrite crystal structure was detected; in the former case, hexagonal δ-FeOOH was obtained. There were no significant differences in the XRD patterns and the M_s in the H_2O_2-oxidized and H_2O_2-non-oxidized samples. The

specific saturation magnetization of the spinel sample was $M_s = 5$ emu/g, whereas the δ-FeOOH sample had $M_s = 4$ emu/g, which is consistent with small average particle sizes, estimated at 3 nm for the spinel sample and at 5.5 nm for the FeOOH sample. It is known that δ-FeOOH is the only FeOOH modification that exhibits a significant magnetization at room temperature [4]. The estimated size of the synthesized particles matches the estimated size of the reverse micelles' "water pools" (2.5 nm in diameter) for the given water volume of the same microemulsion system [5], which might suggest that the reverse micelles indeed acted like encapsulating nano-reactors, limiting the size of the crystallized particles to the sizes of their own pools. This view of the role of reverse micelles in the formation of synthesized material is in agreement with much of the current thinking in this area, although the dynamic interactions among reverse micelles has recently been pointed out as the major influencing factor [2,6].
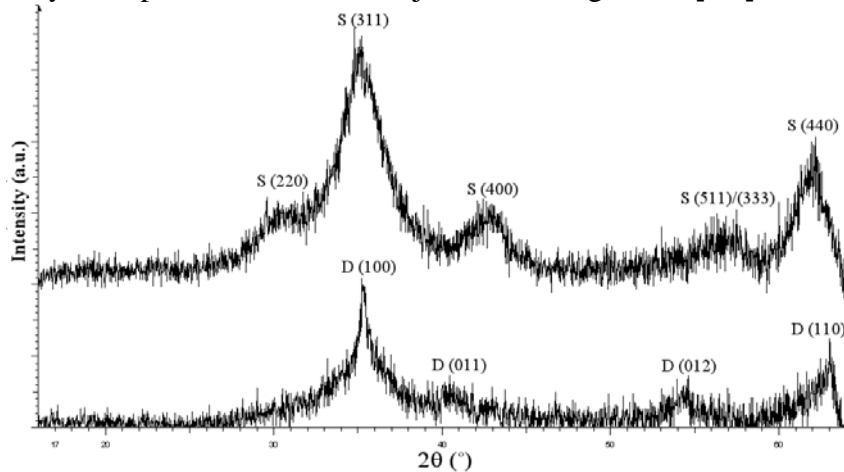

Fig.1. X-ray diffractograms of the powders synthesized by the same precipitation procedure at precipitating pH = 12, with (upper) and without (lower) reverse-micellar microemulsion. The peaks denoted with an S are spinel-derived, whereas the peaks denoted with a D are δ-FeOOH-derived.

The same synthesizing procedures were performed in bulk aqueous solutions in the presence of 3 wt% CTAB, and there were no significant differences in the XRD patterns when compared to the sample synthesized without the presence of CTAB. Therefore, it is not the CTAB that influences the formation of spinel ferrite, rather it is the reverse-micellar structure of the microemulsion.

The influence of pH on the identity and the properties of the microemulsion-assisted synthesized samples

If the precipitating pH in the process of reverse-micellar synthesis exceeded 8, the spinel product was obtained, whereas when the pH was below 8, α-FeOOH was formed as the major product (Fig.2). The specific saturation magnetization (M_s) values of the samples synthesized in the pH range of 8–10 had much lower values of about 1 emu/g, compared to the samples synthesized at pHs of 10–13.5, which had $M_s = 4$–5.5 emu/g. The increase in the M_s values with the increase in the pH of the precipitation is consistent with a similar increase in the samples' crystallinity, which was observed in a previous study [7].
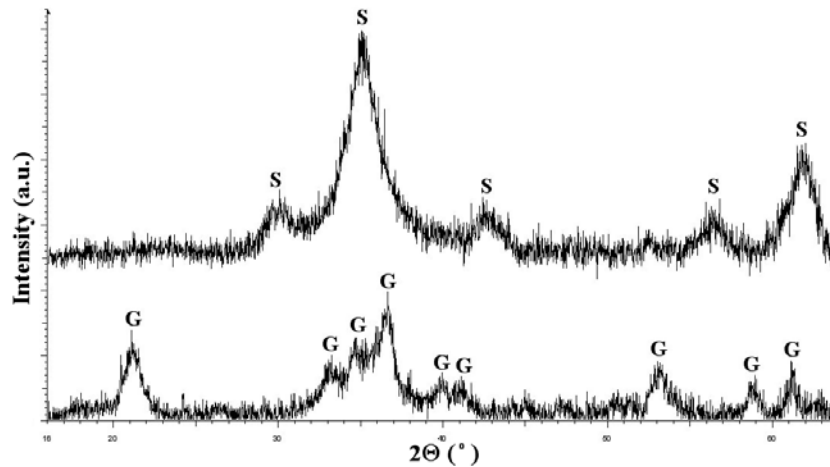
Fig.2. X-ray diffractograms of the sample synthesized in microemulsion at a pH of below 8 (lower) and above 8 (upper). The spinel-derived peaks are denoted with an S, while the goethite-derived peaks are denoted with a G.

The analytically determined stoichiometry of the samples synthesized at a precipitating pH = 9.7 and 12 were $Ni_{0.49}Zn_{0.68}Fe_{1.83}O_4$ and $Ni_{0.48}Zn_{0.73}Fe_{1.79}O_4$, respectively, which suggests that apart from the XRD-determined structure, there were no significant differences in the elemental composition of the samples synthesized at medium and higher precipitating pH values, in spite of the differences in the morphologies. The measured concentration of cations was also the same in both samples, which is another indication that their chemical composition was approximately the same.

a.)   b.)
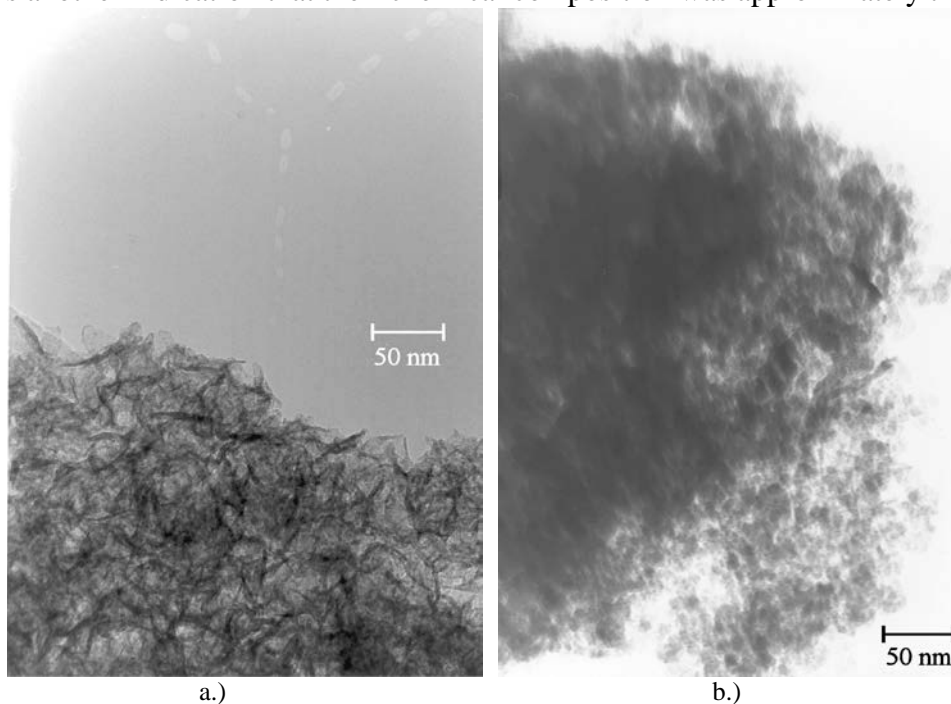
Fig 3. TEM images of the samples synthesized in microemulsion at the precipitating pH = 9 (a) and pH = 11 (b).

TEM images of the samples synthesized at the precipitating pH = 9 and pH = 11 are shown in Fig. 3. Fig 3a shows agglomerates of nanosized acicular particles, whereas

agglomerates of rather spherical particles with sizes of a few nanometers are seen in Fig. 3b. Acicular particles were present to varying degrees in all the samples synthesized at medium pH values (8–11), whereas the samples synthesized at pH ≥ 12 consisted of spherical particles only. We suggest that there are four possible explanations for the existence of acicular particles in the spinel samples:

I) Different modifications of FeOOH are known to represent intermediate compounds during the formation of many spinel-type ferric compounds [8]. A pH < 12 might always induce the formation of acicular α-FeOOH, which might be sufficiently crystalline to be detected with XRD. The isoelectric point, which influences the extent of the aggregation of the growing particles, was found to be around pH = 9. Since a mineral such as FeOOH is regarded as an infinite n-mer extension of $[Fe_2(OH)_2]^{4+}$ [3], the negligible repulsion between the growing particles at around pH = 9 might be the reason for the formation of acicular particles.
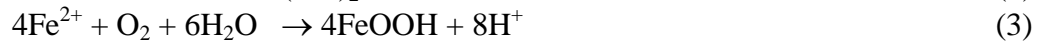
II) It is well known that the rate of transformation of solid phases increases with increasing pH [9,10]. The higher pH usually leads to a higher rate of nucleation, and therefore to a larger number of particles of smaller sizes [11], which might be another reason for the difference in the morphology of the particles synthesized at different values of pH.
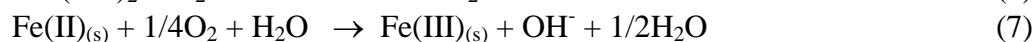
III) The third possibility is that the increased OH^- concentration might substantially eliminate the anions (SO_4^{2-}, Br^-) that might otherwise promote the uniaxial growth of particles by adsorption at specific sites of the growing α-FeOOH particles, or by chemically combining with the particles leading to their specific agglomeration [8]. Sulfate ions, which may promote the appearance of α-phases [9], are only one of the many ionic species known to form complexes with the extremely hydrolyzable ferric ion. During the synthesis of MnZn ferrite using the same chemical procedure, acicular particles were not produced [12], which suggests that Ni^{2+} must be involved in the mechanism of the uniaxial growth of the particles.

IV) The fourth possibility is that the lower pH values under given experimental conditions favor the formation of elliptical or very long, rod-shaped reverse micelles, which are known to exist in microemulsion systems that comprise CTAB as the surfactant [13,14,15]. It is also known that an alkali substance [16], salts [13] or co-surfactant [17,18], such as 1-hexanol [19], might induce a spherical-to-worm-like transition. Elliptical and spherical CTAB micelles are known to be able to co-exist [20], which might explain why the samples synthesized at medium pH values (pH = 10–11) comprised not just acicular, but spherical particles as well.

The proposed chemical pathway and the effects of compartmentalizing the reactants

A simplified chemical pathway that leads to the formation of NiZn ferrite from the starting process of the precipitation of divalent precursor cations might be summarized as follows:

$$Fe^{2+} + 1/4 O_2 + H^+ \rightarrow Fe^{3+} + 1/2 H_2O \qquad (1)$$
$$Fe^{2+} + 2OH^- \rightarrow Fe(OH)_2 \qquad (2)$$
$$4Fe^{2+} + O_2 + 6H_2O \rightarrow 4FeOOH + 8H^+ \qquad (3)$$

$$Ni^{2+} + Zn^{2+} + 4OH^- \rightarrow Ni(OH)_2 + Zn(OH)_2 \qquad (4)$$

$$Fe^{3+} + 3H_2O \rightarrow Fe(OH)_3 + 3H^+ \qquad (5)$$
$$4Fe(OH)_2 + O_2 \rightarrow 4FeOOH + 2H_2O \qquad (6)$$
$$Fe(II)_{(s)} + 1/4O_2 + H_2O \rightarrow Fe(III)_{(s)} + OH^- + 1/2H_2O \qquad (7)$$

$$Fe(OH)_3 \rightarrow FeOOH + H_2O \qquad (8)$$

Only if pH > 8,
$$2Fe(III)_{(s)} + 1/2Ni(OH)_2 + 1/2Zn(OH)_2 \rightarrow Ni_{0.5}Zn_{0.5}Fe_2O_4 + 2H_2O \qquad (9)$$
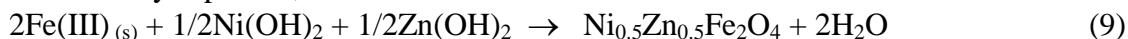
When H_2O_2 is used as an oxidant, then the following reaction also applies:
$$Fe^{2+} + H_2O_2 \rightarrow Fe^{3+} + OH^- + OH^. \qquad (10)$$

The chemical reactions described by equations 1-4 are actuated immediately after the moment of mixing two microemulsions, whereas the first microemulsion comprises aqueous solution of precursor cations and the other microemulsion carries precipitating agent in the water 'pools' of its reverse micelles. The reactions described by equations 5-8 describe processes that lead to the completion of oxidation of ferrous ions, and their precipitation within the range of their solubility limits. The initial precipitate should mostly comprise amorphous gel of divalent precursor cations hydroxides. Oxidized ferric ions are then at first incorporated together with unoxidized ferrous ions in the intermediate compound of Green Rust II (which is known to present an intermediate when using sulphate precursor salts [21]). The intermediate precipitate of Green Rust II, later with subsequent oxidation of remaining ferrous ions, transforms in the precipitate of certain form of FeOOH, depending on the pH value of the solution, as well as on possibly catalyzing effects of certain dissolved ions.

We believe that the reason why the desired ferrite was formed only in the microemulsion, and not in the absence of the microemulsion, is that the compartmentalization of the reactants in small, nanosized droplets of water increases the rate of oxidation of ferrous ions, and thus makes the formation of mixed zinc ferrite likely, even for a relatively short aging time of 1 hour. The reason why δ-FeOOH was only formed in bulk conditions is that the oxidation was probably not as fast as in the microemulsion from the very beginning, but only after the precipitate of $Fe(OH)_2$ was already formed. This statement is based on observing the color changes in both the bulk and the microemulsion conditions. The color of the microemulsion changed from black to orange approximately 5 minutes after the precipitation reaction was initiated, which is a result of the formation of Fe^{3+} ions. In contrast, the color of the bulk solution remained black throughout the whole aging experiment, and turned orange only if a foreign oxidizing agent such as H_2O_2 was added. It has been reported that the rate of oxidation of Fe^{2+} and the subsequent formation of needle-like FeOOH particles by spontaneous air oxidation was from 100 to 1000 times faster in reverse micelles than in a bulk solution [22]. In the case of certain iron complexes, a 2–10-fold increase in the rate of dissociation was measured in comparison to the pure aqueous solution (cited in [23]). It is possible that the reason for the faster rate of Fe^{2+} oxidation in reverse micelles compared to the bulk conditions might lie in the atypical structure of water as a solvent in reverse

micelles. It was suggested that the increase in hydrogen bonding between water molecules in a thin layer neighboring to surfactants may form a field where easy transfer of electrons from Fe^{2+} to Fe^{3+} occurs by a tunnelling effect [22], whereby the excess electrons will be consumed in aqueous solution to produce hydroxide ions in the presence of dissolved oxygen. The oxidation of Fe^{2+} with the decomposition of H_2O is, by considering thermodynamic data, proven to be an energetically favorable process.

The precipitation reaction should be slower in a reverse-micellar medium, when considering the necessary coupling of the rate constant of the chemical reaction and the rate constant of the fusion of reverse micelles, which must happen prior to the particular reaction [6]. The slower rate of the precipitation when the synthesis is performed within reverse micelles compared to the bulk conditions could be another effect that would, together with the faster rate of oxidation in the former case, lead to better conditions for the formation of ferrite in the microemulsion only, and not in the bulk solution. Oxidation is known to proceed much faster when the oxidized species are diluted than when they are precipitated, which is the reason why decreasing the rate of precipitation by compartmentalizing the reactants increases the rate of oxidation. On the other hand, Fe^{2+} and Fe^{3+} yield insoluble hydroxide phases in alkaline solutions, which decreases the redox potential for the oxidation reaction to about 0.52 V, and increases the rate of oxidation of the diluted ferrous ions [24]. In other words, the oxidation of Fe^{2+} is driven forward by the removal of Fe^{3+} ions from the solution in form of hydroxide precipitate. Considering redox-potentials, it is obvious that the precipitation of ferric ions increases the rate of oxidation of dilluted ferrous ions. This might explain why the spherical and more magnetic particles were obtained at higher pH values when oxidation occurred faster due to the faster precipitation and the whole transition of FeOOH to ferrite happened in a faster way.

The influence of the initial pH on the chemical pathway of reverse-micellar synthesis

A typical pH vs. aging-time dependence for the final precipitating pH = 12 is shown in Fig. 4a. The sudden decrease in the pH value just as the precipitation is initiated is due to the precipitation of precursor cations and the subsequent decrease of the OH⁻ concentration (eq. 2, 3, 4) in the colloid solution, and the hydrolysis reactions of the oxidation species (eq. 3, 5).
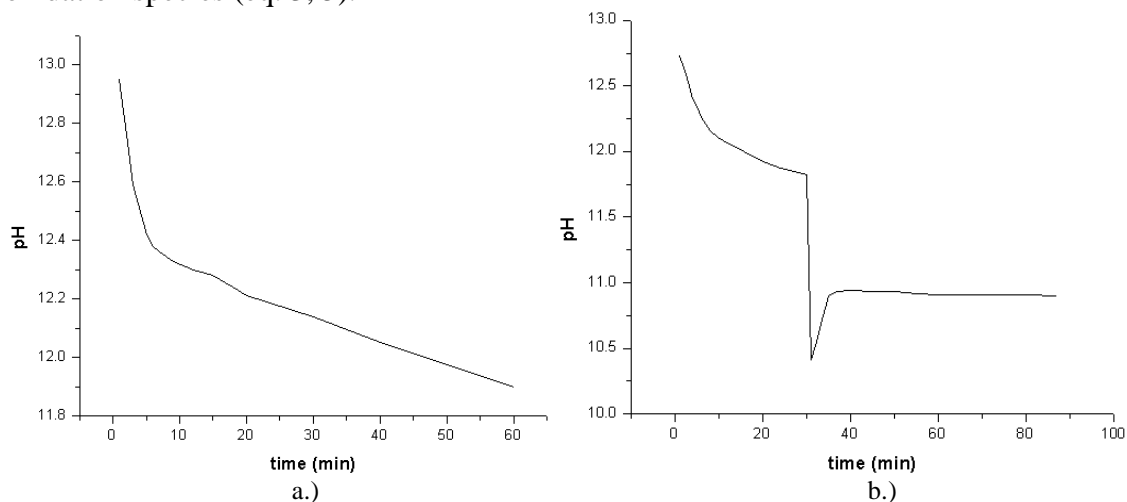

a.)   b.)

Fig. 4. Dependence of pH value versus aging time for the higher precipitating pH value case for the H_2O_2-non-oxidized (a) and the H_2O_2-oxidized microemulsion-assisted synthesized sample (b).

Changes in the initiating pH of the precipitation bring about two opposite effects: with increasing the initial pH value, the OH^- concentration increases, which favors faster rates of oxidation, but the precipitation proceeds faster too, which leads to longer times needed to complete the Fe^{2+} oxidation process [9]. With the proposed slowing down of the precipitation reaction due to coupled intermicellar exchange to the rate of the chemical reaction itself, it is possible that the former effect – oxidation – is favored, which consequently favors the faster formation of NiZn ferrite, or its formation at all. The shorter the time needed for Fe ions to precipitate, the faster the oxidation occurs. A sudden decrease in pH at the moment when the H_2O_2 is introduced into the microemulsion (Fig. 4b) is due to its immediate dissociation in an alkali medium:

$$H_2O_2 \rightarrow H^+ + HO_2^- \tag{11}$$

The reaction proceeds:

$$HO_2^- + H_2O + 2e^- \rightarrow 3OH^- \tag{12}$$

which implies an increase in pH that follows.

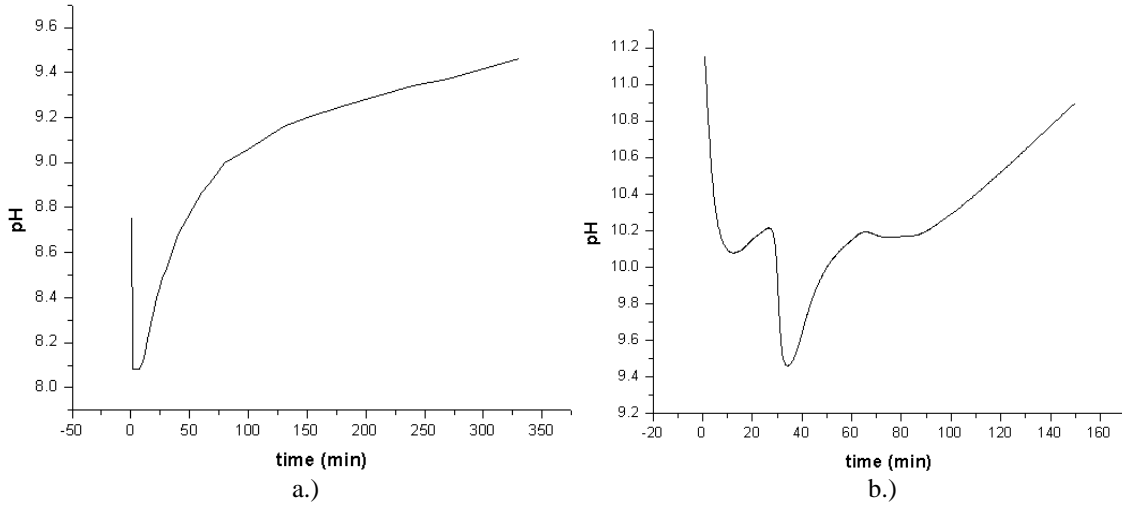a.)   b.)

Fig.5. Dependence of pH value versus aging time for the lower precipitating pH value case for the H_2O_2-non-oxidized (a) and the H_2O_2-oxidized microemulsion-assisted synthesized sample (b).

It was observed that if the pH values during the process do not fall below pH = 10, the pH value constantly decreases and therefore the equilibrium state is reached with the pH vs. time curve sloping downwards, as shown in Fig. 4. On the other hand, when the pH value of the solution falls below approximately 10 (Fig. 5), a range of increasing pH values would follow a decreasing pH value range, and equilibrium would be reached with the pH vs. time curve sloping upwards. The decreasing pH with aging time is most probably a sign of the oxidation of ferrous species in the solution, i.e., in the aqueous phase of the microemulsion, whereas the increasing trend of the dependence of pH versus time is a sign of the oxidation of ferrous ions already precipitated in the form of a colloidal precipitate (eq. 7). This suggests that in the cases of higher pH values shown in Fig. 4, both precipitation and oxidation were favored from the very start of the precipitation reaction, whereas the trend of increasing pH vs. aging time at medium and lower precipitating pH values suggests that the precipitation of precursor cations in the

form of hydroxides was favored over the rate of oxidation, so that after the cations were precipitated, oxidation reactions continued. This difference in the precipitation rate depending on the pH value is to be expected when considering the fact that the higher pH within the reverse micelles would lead to a greater repulsion between them and to a consequently slower rate of their merging.

Conclusions

Different mechanisms for the formation of NiZn ferrite, which was to have the $Ni_{0.5}Zn_{0.5}Fe_2O_4$ stoichiometric formula, in bulk solution, as well as in a reverse-micellar $CTAB/1$-hexanol/H_2O microemulsion at lower and higher precipitating pH values were discussed in terms of the evidence from XRD patterns, different particle morphologies shown in TEM images, different visual appearance throughout the aging time of the precipitate and different changes in pH of the synthesizing microemulsion versus aging time. When performing the same chemical procedure with and without the reverse micelles, different products were obtained: nanocrystalline NiZn ferrite with an analytically determined stoichiometry of $Ni_{0.5}Zn_{0.7}Fe_{1.8}O_{3.9}$ in the former case, and δ-FeOOH in the latter case. Faster rates of oxidation and slower rates of precipitation when the synthesis was performed in reverse micelles rather than in bulk conditions were suggested as the reason for the difference in the chemical identity of the final product for these two chemical procedures. If the pH of the precipitation decreases below 8 during the aging procedure in the microemulsion, goethite was obtained as the main product. Otherwise, NiZn ferrite with a lower magnetization and acicular particles were obtained in the precipitating pH range of 8–10, and higher magnetization and spherical particles in the precipitating pH range of 11–13.5. The formation of acicular particles below a certain range of the precipitating pH was discussed and related to the presence of the acicular form of FeOOH as the intermediate phase in the chemical pathway of the formation of NiZn ferrite, and on the oxidation reactions performed over already precipitated ferrous ions in the lower pH case, whereas the oxidation is thought to be performed over dissolved ferrous ions in the higher pH value case.

Acknowledgements

References

1. D. O. Yener, H. Giesche – "Synthesis of Pure and Manganese-, Nickel-, and Zinc-Doped Ferrite Particles in Water-in-Oil Microemulsions", Journal of the American Ceramic Society **84** (9) 1987-95 (2001).
2. R. Zana, J. Lang – "Dynamics of Microemulsions", in Microemulsions: Structure and Dynamics, edited by S. E. Friberg and P. Bothorel, Boca Raton: CRC Press, 153 – 72 (1987).
3. S. T. Martin – "Properties and Dissolution of Iron and Manganese Oxides", Chapter 4 of Environmental Catalysis, edited by V. H. Grassian (2003).

4. L. H. Perng, I.-C. Tung, T. S. Chin – "Synthesis and Properties of Nanocrystalline δ-FeOOH", Journal de Physique IV France **7**, C1-519-20 (1997).
5. E. Rodenas, M. Valiente – "The Determination of Some Physical Properties of Reverse CTAB Micelles in 1-Hexanol", Colloids and Surfaces **62**, 289 – 95 (1992).
6. U. Natarajan, K. Handique, A. Mehra, J. R. Bellare, K. C. Khilar – "Ultrafine Metal Particle Formation in Reverse Micellar Systems: Effects of Intermicellar Exchange on the Formation of Particles", Langmuir **12**, 2670 – 78 (1996).
7. V. Uskoković, M. Drofenik – "Synthesis of Nanocrystalline Nickel-Zinc Ferrites via a Microemulsion Route", Materials Science Forum **453 – 4**, 225 – 30 (2004).
8. G. Bate – "Recording Materials", in Ferromagnetic Materials, edited by E. P. Wohlfarth, North-Holland Publishing Company (1980).
9. C. Domingo, R. Rodriguez-Clemente, M. A. Blesa – "The Pathways to Spinel Iron Oxides by Oxidation of Iron (II) in Basic Media", Materials Research Bulletin **26**, 47 – 55 (1991).
10. T. Sugimoto, E. Matijević – "Formation of Uniform Spherical Magnetite Particles by Crystallization from Ferrous Hydroxide Gels", Journal of Colloid and Interface Science **74** (1), 227 – 43 (1980).
11. G. Wang, G. Whittaker, A. Harrison, L. Song – "Preparation and Mechanism of Formation of Acicular Particles by Decomposition of Ferric and Ferrous Salts in Aqueous Solution Using Microwave Radiation", Materials Research Bulletin **33** (11), 1571 – 79 (1998).
12. A. Košak, D. Makovec, A. Žnidaršič, M. Drofenik – "Preparation of MnZn-Ferrite with Microemulsion Technique", Journal of the European Ceramic Society **24** (6) 959 – 62 (2003).
13. Y. Liu, W. Wang, Y. Zhan, C. Zheng, G. Wang – "A Simple Route to Hydroxyapatite Nanofibers", Materials Letters **56**, 496 – 501 (2002).
14. S. Xu, H. Zhou, J. Xu, Y. Li – "Synthesis of Size-Tunable Silver Iodide Nanowires in Reverse Micelles", Langmuir **18**, 10503 – 4 (2002).
15. M. P. Pileni, A. Hammounda, I. Lisiecki, L. Motte, N. Moumen, J. Tanori – "Control of the Size and Shape of Nanoparticles", in Fine Particles Science and Technology, edited by E. Pelizzetti, Kluwer Academic Publishers, 413 – 29 (1996).
16. F. G. Sanchez, C. C. Ruiz – "Intramicellar Energy Transfer in Aqueous CTAB Solutions", Journal of Luminiscence **69**, 179 – 86 (1996).
17. X. Fang, C. Yang – "An Experimental Study on the Relationship between the Physical Properties of CTAB/Hexanol/Water Reverse Micelles and ZrO_2-Y_2O_3 Nanoparticles Prepared", Journal of Colloid and Interface Science **212**, 242 – 51 (1999).
18. J. Yang – "Viscoelastic Wormlike Micelles and their Applications", Current Opinion in Colloid & Interface Science **7**, 276 – 81 (2002).
19. B. Lindman, H. Wennerstrom – "Micelles. Amphiphile Aggregation in A queous Solution" in Topics in Current Chemistry **87**: Micelles, Springer-Verlag Berlin Heidelberg (1980).

20. Z. Lin, J. J. Cai, L. E. Scriven, H. T. Davis – "Spherical-to-Wormlike Micelle Transition in CTAB Solutions", Journal of Physical Chemistry **98**, 5984 – 93 (1994).

21. J. Dufour, J. O. Marron, C. Negro, R. Latorre, A. Formoso, F. Lopez-Mateos – "Mechanism and Kinetic Control of the Oxyprecipitation of Sulphuric Liquors from Steel Pickling", Chemical Engineering Journal **68**, 173 – 87 (1997).

22. K. Inouye, R. Endo, Y. Otsuka, K. Miyashiro, K. Kaneko, T. Ishikawa – "Oxygenation of Ferrous-Ions in Reversed Micelle and Reversed Micro-Emulsion", Journal of Physical Chemistry **86** (8), 1465 – 69 (1982).

23. J. Sjöblom, R. Lindberg, S. E. Friberg – "Microemulsions – Phase Equilibria Characterization, Structures, Applications and Chemical Reactions", Advances in Colloid and Interface Science **95**, 125 – 287 (1996).

24. I. Filipović, S. Lipanović – "Opća i anorganska kemija", Školska knjiga, Zagreb (1985).

25. T. Wang, Y. Jin, Z. Wang, Z. Yu – "A Study of the Morphology of the Goethite Crystallization Process", Chemical Engineering Journal **69**, 1-5 (1998).

26. T. Sugimoto, A. Muramatsu – "Formation Mechanism of Monodispersed α-Fe_2O_3 Particles in Dilute $FeCl_3$ Solutions". Journal of Colloid and Interface Science **184**, 626 – 38 (1996).